Wavelength Locking and Thermally Stabilizing Microring Resonators Using Dithering Signals

Kishore Padmaraju, *Student Member, IEEE*, Dylan F. Logan, Takashi Shiraishi, *Member, IEEE*, Jason J. Ackert, Andrew P. Knights, and Keren Bergman, *Fellow, IEEE, Fellow, OSA*

***Abstract*—The bandwidth bottleneck looming for traditional electronic interconnects has driven the consideration of optical communications technologies as realized through the complementary metal-oxide-semiconductor-compatible silicon nanophotonic platform. Within the silicon photonics platform, silicon microring resonators have received a great deal of attention for their ability to implement the critical functionalities of an on-chip optical network while offering superior energy-efficiency and small footprint characteristics. However, silicon microring-based structures have a large susceptibility to fabrication errors and changes in temperature. Integrated heaters that provide local heating of individual microrings offer a method to correct for these effects, but no large-scale solution has been achieved to automate their tuning process. In this context, we present the use of dithering signals as a broad method for automatic wavelength tuning and thermal stabilization of microring resonators. We show that this technique can be manifested in low-speed analog and digital circuitry, lending credence to its ability to be scaled to a complete photonic interconnection network.**

***Index Terms*—Frequency locked loops, multi-processor interconnection, optical interconnects, optical resonators.**

I. Introduction

GROWING bandwidth needs are motivating the replacement of traditionally electronic links with optical links for applications as diverse as data centers, supercomputers, embedded computing processor-memory interconnects, and fiber-optic access networks [1], [2]. For applications such as these, the silicon photonics platform has received significant attention because of its ability to deliver the necessary bandwidth, and by leveraging its compatibility with complementary metal-oxide-semiconductor (CMOS) fabrication, at a potential economy of scale. In particular, silicon microring resonator based devices exhibit leading metrics on size density, energy-efficiency, and ease of wavelength-division-multiplexed (WDM) operation [3].

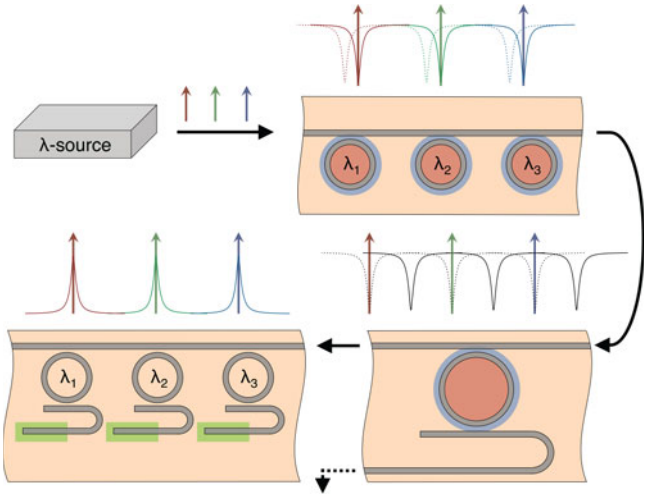

Fig. 1. An optical link composed of microring-based devices. A wavelength source (λ-source) is modulated by multiplexed microring modulators (doped in a diode configuration to enable fast carrier-induced resonance shifts). A microring switch can then route the entire set of signals appropriately before it is received by a demultiplexing microring array.

Fig. 1 illustrates a portion of an envisioned microring-based photonic network that would be used for transcribing electrical data signals into the optical domain, transmitting and routing them as necessary, and converting the optical signals back to the electrical domain at the termination of the link. The beginning of the link consists of a multi-wavelength laser source. These laser wavelengths are individually modulated by cascaded microring modulators in a multiplexed configuration. The entire set of signals can then be routed as necessary by microring-based switches. Finally, they are received by a microring array that demultiplexes the individual signals before receiving them on independent photodetectors.

The basic configuration of Fig. 1 is but one of a myriad of proposed possibilities for photonic networks enabled by microring-based devices, with more complex network designs fully leveraging the unique capabilities of microrings [4], [5]. However, these proposed microring-based photonic networks currently face severe challenges in the path towards commercial realization. Specifically, the relatively high thermo-optic coefficient of silicon combined with the wavelength selectivity of microring

Manuscript received July 11, 2013; revised November 6, 2013; accepted December 6, 2013. Date of publication December 10, 2013; date of current version December 27, 2013. This work was supported in part by the National Science Foundation and Semiconductor Research Corporation under Grant ECCS-0903406 SRC Task 2001. This work was also supported by the Natural Sciences and Engineering Research Council of Canada. The work of K. Padmaraju was supported by an IBM/SRC PhD fellowship.

K. Padmaraju and K. Bergman are with the Department of Electrical Engineering, Columbia University, New York, NY 10027 USA (e-mail: kpadmara@ee.columbia.edu; bergman@ee.columbia.edu).

D. F. Logan is with the Ranovus Inc., Ottawa, ON A6 K1A 0R6, Canada (e-mail: dylan@ranovus.com).

T. Shiraishi is with the Department of Electrical Engineering, Columbia University, New York, NY 10027 USA, and also with the Photonics Laboratory, Fujitsu Laboratories Ltd., Kanagawa 2430197, Japan (e-mail: ts2821@columbia.edu).

J. J. Ackert and A. P. Knights are with the Department of Engineering Physics, McMaster University, Hamilton, ON L8S 4L8, Canada (e-mail: ackertjj@mcmaster.ca; aknight@mcmaster.ca).

Color versions of one or more of the figures in this paper are available online at http://ieeexplore.ieee.org.

Digital Object Identifier 10.1109/JLT.2013.2294564

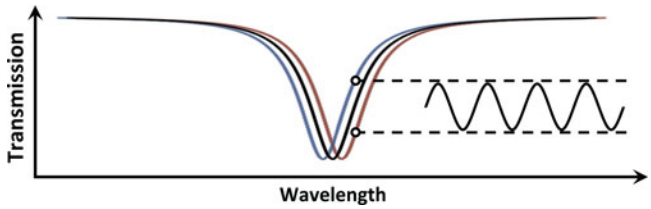

Fig. 2. A small dither signal, applied thermally to the microring resonator, results in a small modulation of the optical signal.

resonators lends them susceptible to changes in temperature and laser wavelength. Additionally, fabrication tolerances will likely result in microring resonators that are initially offset from their designed operating wavelength.

The dominant method of resolving these problems is to use energy-efficient integrated heaters to tune and stabilize the microring resonance to the laser wavelength [6]. While demonstrations of manual tuning validate the functionality of these heaters, for commercial implementations an energy-efficient and scalable solution to lock and stabilize microring resonators is required.

There have been several attempted solutions for wavelength locking and thermally stabilizing microring resonators [7]–[11]. However, no prior demonstrated system has satisfied all required criteria, that is, a system that is scalable, low-cost, energy-efficient, immune to fluctuations in optical power, compatible with WDM implementation, and does not require additional photonic structures. Recognizing the limitations of traditional techniques in addressing the above listed criteria, we have pioneered a novel method of locking and stabilizing microring resonators.

The underlying principle of our method is to use dithering signals to break the symmetry of the microring resonator [12]. For most applications, the minimum transmission point of the microring resonance is aligned with the laser wavelength it is routing and detecting. In this configuration, it is difficult to lock the microring resonance to the laser wavelength by measuring just the optical power transmission, because the direction of resonance shift is ambiguous in relation to the transmission of optical power. Historically, to overcome this, methods such as the Pound–Drever–Hall (PDH) technique have been used to generate anti-symmetric error signals that can be utilized by closed-loop feedback controllers [13]. However, the details of the PDH technique are not suitable for the scenario of wavelength locking a microring resonator, and we look towards the use a dithering signal for the purpose of generating the desired anti-symmetric error signal.

Fig. 2 illustrates the dithering mechanism (applied thermally), whereby a small modulation is applied to the local temperature of the microring in order to produce a small modulation of the optical signal. The generated optical modulation will either be in-, or out-of-phase with the driving signal, depending on which side of the resonance the laser wavelength is offset. By mixing the modulated optical signal with the driving dithering signal this information can be recovered as shown in (1), where f_D is the frequency of the dithering signal, and ϕ is the relative phase

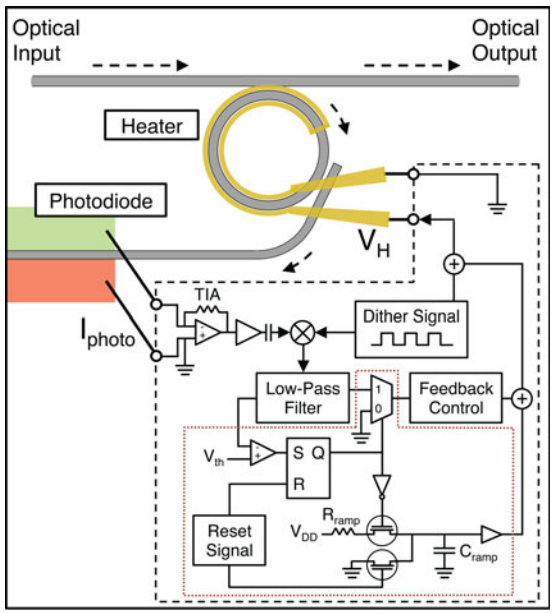

Fig. 3. A schematic of the device used in this experiment (not to scale). The off-chip electronics interfacing with the integrated photonic elements are shown in the dashed box. Highlighted in the red box is the circuitry devoted to wavelength locking.

(0 or π) of the modulated optical signal

$$\cos(f_D t) \otimes \cos(f_D t + \phi) = \frac{1}{2}[\cos(2f_D t + \phi) + \cos(\phi)]. \tag{1}$$

The higher harmonic can be filtered, leaving the sign of the dc component $\{\cos(\phi)$ term$\}$ as an indication of the location of the resonance relative to the optical signal. The end product of this process is the desired anti-symmetric error signal.

II. Device and Experimental Setup

The device we used to demonstrate our method is illustrated in Fig. 3, and consists of a 15-μm radius silicon microring resonator (on a SOI platform). A thin film titanium-based heater is situated directly above the microring, separated from the microring by 1 μm of oxide. The drop port of the microring terminates in a defect-enhanced silicon photodiode, enabling the monitoring of the optical power dropped into the microring [14].

The off-chip electronics implementing the thermal dithering system are shown in the dashed box of Fig. 3. The electronics consist of low-speed (<20-MHz bandwidth) analog and digital ICs. The dithering signal is chosen to be higher in frequency than the thermal fluctuations it is monitoring.

The optical signal, modulated by the thermal dithering, generates a photocurrent on the integrated silicon photodiode. The photocurrent is converted to a voltage using a transimpedance amplifier (TIA), and then furthered amplified. An analog multiplier IC (AD 633) is used to then mix the amplified signal with the driving dithering signal. A low-pass *RC* filter is used to suppress the ac component of the mixed product. The result of this process is the generation of an anti-symmetric error signal

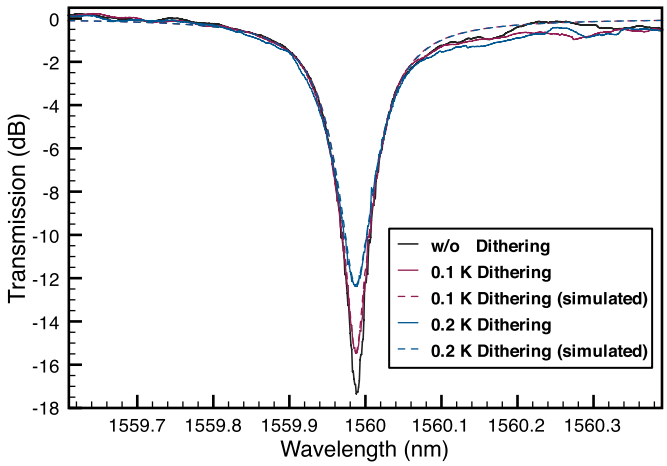

(a)

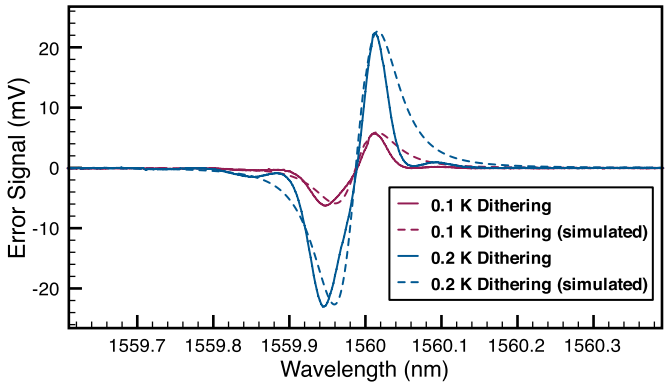

(b)

Fig. 4. (a) The microring resonance as it is subjected to thermal dithering signals of varying magnitude (simulations in dashed). (b) The corresponding generated error signals (simulations in dashed).

that can then be used for the purpose of initializing (wavelength locking) and thermally stabilizing the microring resonator.

A. Generated Anti-Symmetric Error Signal

The use of the thermal dithering signal has the consequence of reducing the extinction ratio of the microring resonance. In Fig. 4(a), the simulated and measured resonances of the microring resonator (Q of $\sim$14,000) are plotted for square-wave thermal dithering signals of magnitude 0.1 and 0.2 K. A larger thermal dither will result in a larger reduction of the extinction ratio. Fig. 4(a) shows the un-dithered resonance having an original extinction ratio of 17.3 dB. For thermal dithering of magnitude 0.1 K and 0.2 K the reduction in extinction ratio was measured to be 1.9 and 4.8 dB, respectively. Simulations produced identical results (Fig. 4(a)).

While a larger thermal dither results in a larger reduction in extinction ratio, it has the advantage of producing a stronger error signal. Fig. 4(b) plots the simulated and measured waveforms of the generated error signal.

The anti-symmetric response of the error signal [see Fig. 4(b)] clearly distinguishes between the red and blue sides of the microring resonance. Furthermore, the zero crossing of the monotonic slope is located at the resonance minimum. Hence, a feedback controller can easily stay locked to the zero crossing in order to lock the microring resonance with the laser wavelength.

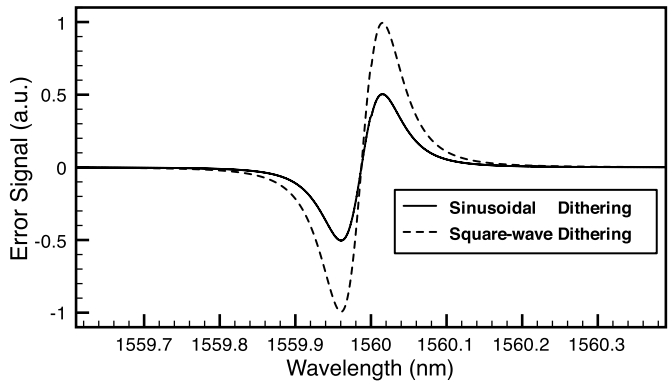

Fig. 5. Simulations of the generated error signal contrast the use of a square-wave dithering signal versus the use of a sinusoidal dithering signal.

While a larger error signal makes the system more robust against noise, we found that the smaller 0.1 K dithering signal generated a sufficient error signal for locking and stabilizing the microring resonator. All further results described in this paper were done using a dithering signal of magnitude 0.1 K.

B. Optimization of the Error Signal

In our experimental implementation we utilized a square-wave dithering signal rather than the sinusoidal dithering signal described in (1). In theory, the dithering signal can be composed of any periodic waveform. However, the square-wave offers the advantage of being able to be synthesized easily in electronic circuitry. Additionally, the mixed product of (ideal) square-waves will produce a pure dc component and none of the higher harmonic components that are eventually filtered (see the Appendix). This has the consequence of producing a larger error signal for dithering signals of equivalent magnitude. Fig. 5 graphs simulations of the generated error signals when using an ideal square-wave dithering signal versus using an ideal sinusoidal dithering signal. As can be seen from the graph, the square-wave dithering signal generates an error signal that is twice as large in magnitude.

C. Immunity to Power Fluctuations

A significant advantage of the generated error signal is that it is relatively immune to changes in the optical power of the signal. In future microring-based optical networks it is envisioned that optical paths can be reconfigured as necessary to address dynamic bandwidth allocation requirements. The insertion loss characteristics of optical paths will change as they are re-provisioned, yielding uncertainty in the optical power reaching any given microring resonator.

As Fig. 6 shows the generated error signals will change in magnitude following variations in optical power. Additionally, the slope of the error signal will also vary. However, a robust feedback controller (one that is able to contend with the change

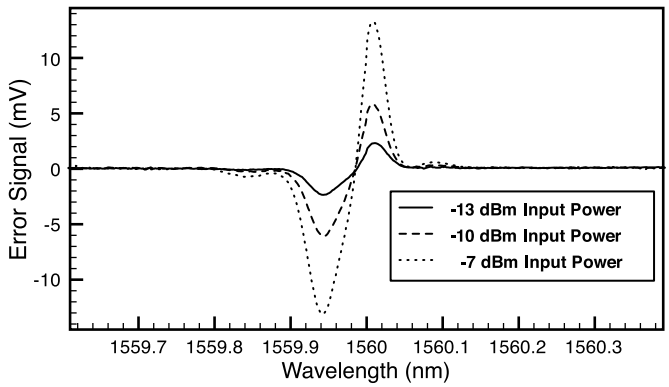

Fig. 6. The measured error signals when a 0.1 K thermal dithering is applied and the optical power of the laser into the chip is varied.

in slope of the error signal) will be able to maintain the locking between the microring resonator and laser wavelength because the zero crossing of the error signal remains constant.

It should also be noted that, as demonstrated, these error signals can be generated with a relatively weak optical signal reaching the photodetector. The fiber-to-fiber coupling loss of the chip was measured to be $\sim$20 dB; assuming symmetric coupler and waveguide losses, the power reaching the photodetector for the measured error signals in Fig. 6 is then less than -20 dBm. This figure covers the lowest optical powers that would be present in a silicon photonic link due to the sensitivity limit on current photodetectors [3].

D. *Effect on Data Signals*

For use in data applications, it is critical that the dithering of the microring resonance does not negatively impact the integrity of the optical data signals. To test this, we simulated 10 Gb/s optical data signals as they are routed from the input port, through the microring, and into the drop port of a dithered microring resonator (a microring in the demultiplexing configuration). Fig. 7 shows the simulated eye patterns of the received signal when a dithering signal of magnitude of 0.1 and 0.2 K was applied to the microring, as well as when no dithering signal was applied (as stated before, a 0.1 K dithering magnitude was sufficient for experimentally locking and thermally stabilizing the microring resonator). In these simulations, we modeled the microring resonator to have the same characteristics (extinction ratio and Q-factor) as the microring resonator we worked experimentally with [see Fig. 4(a)].

As expected, and as evidenced by the simulated eye patterns, the dithering has the effect of broadening only the '1' level of the optical signal. However, this broadening is minimal, resulting in eye closures of only 0.3% and 1.6% when using dithering signals of 0.1 and 0.2 K, respectively. For small deterministic eye closures such as this, the power penalties can be directly correlated as being 0.01 and 0.07 dB, respectively. Power penalties of this magnitude are well within the optical link budgets for microring-based links [3], and hence will not impede the use of the dithering technique for data applications.

Finally, it should be noted that the error signal generated from a modulated signal will be smaller than the error signal generated from an unmodulated signal. This is due to the broadened spectrum of the modulated signal. Our simulations show that the error signal generated from a 10-Gbps NRZ signal will be 20% smaller than an error signal generated from an unmodulated signal (when using a microring resonator with the prior discussed parameters).

III. Wavelength Locking

The first application of the generated error signal is in the process of tuning the microring resonator such that it is aligned in resonant wavelength with the laser source. Denoted as wavelength locking, this is a critical functionality for any given microring-based platform as the lasers and microring resonators will be initially offset in wavelength due to fabrication tolerances or changes in the ambient temperature.

The electronic circuitry devoted to the wavelength locking process is detailed in Fig. 3 (outlined by the red box). The functionality of this circuitry is succinctly described in the state diagram of Fig. 8. A simple reset signal is used to trigger the ramping of the voltage applied to the integrated heater. As the microring is tuned to the laser wavelength the error signal will trip the system into the hold state, in which the feedback controller is activated and the microring is locked and stabilized against further drifts in temperature or laser wavelength. Additional logic can be added to reset and re-attempt the wavelength locking should it fail on its initial attempt.

The optical spectrum analyzer traces in Fig. 9 demonstrate the system locking a microring resonator to a laser (an ASE source is used to background image the microring's resonance). Initially, the microring resonance is at $\sim$1559.2 nm, and the laser is offset at $\sim$1560 nm. Over the course of 50 s, the microring is tuned higher in wavelength until the control system detects the error signal and establishes the lock. To record the optical traces of Fig. 9, the ramp speed (rate at which the tuning occurs) of the system was drastically reduced, such that the wavelength locking would occur over the course of seconds. In subsequent trials, the ramp speed was increased to achieve wavelength locking in the $\sim$ms time frame. In future implementations, the speed of the dithering signal can easily be increased to $>$1 MHz to allow the wavelength locking to occur in the $\sim\mu$s time frame. At that point, the fundamental limits on the speed of the wavelength locking will be determined by the initial offset between the microring resonance and the laser wavelength, and the rate at which the integrated heater can tune the temperature of the resonator.

Fig. 10 shows an oscilloscope measurement of the heater voltage during the wavelength locking process. Here, the ramp speed has been decreased to allow locking in the $\sim$ms regime. The graph of Fig. 10 has been annotated with the stages of the state machine, with the period (I) designating the heater voltage while the system is in the reset state, (II) designating the period in which the voltage is ramped, and (III) designating the wavelength-locked hold state, which occurs once the microring resonator and wavelength become aligned.

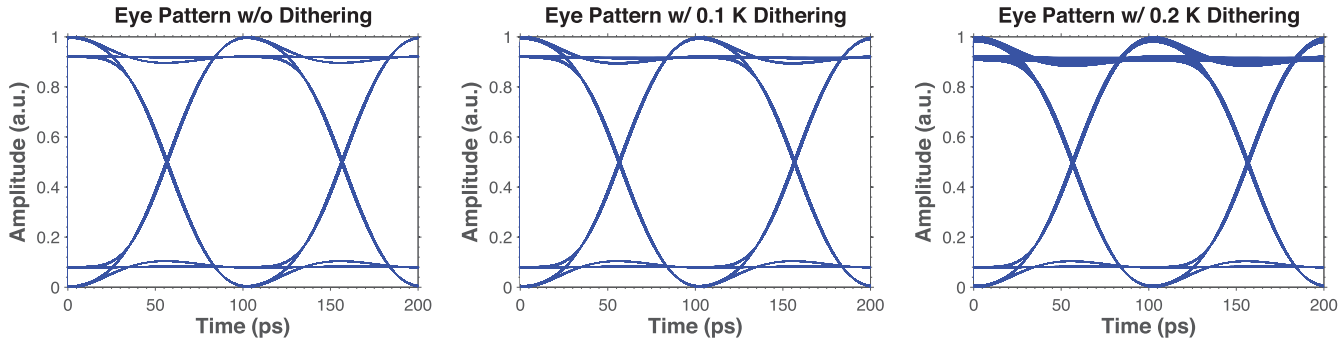

Fig. 7. Simulations of the eye pattern of a 10 Gb/s optical signal propagating through a microring with no dithering (left), and dithering of magnitudes 0.1 K (middle) and 0.2 K (right).

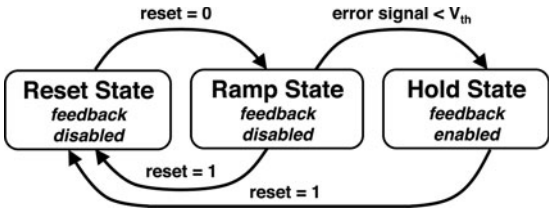

Fig. 8. A state diagram describing the functionality of the wavelength locking circuitry (red box, Fig. 3).

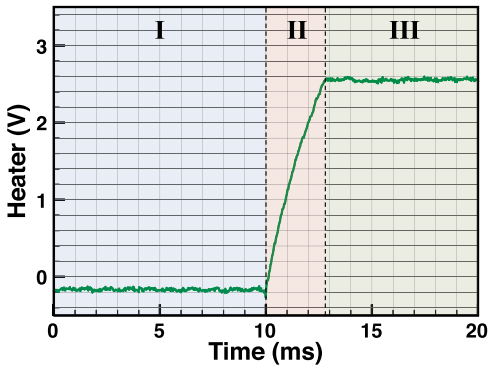

Fig. 10. Oscilloscope trace of the heater voltage as the microring is wavelength locked to the laser source. Annotated are the reset state (I), ramp state (II), and hold state (III).

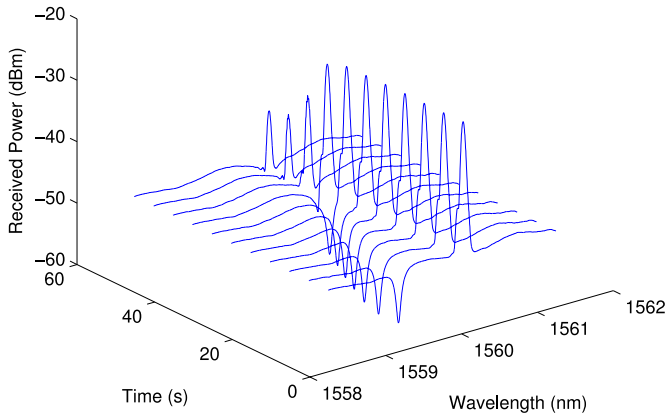

Fig. 9. Optical traces show the microring resonance being tuned and wavelength locked to a laser source.

IV. Thermal Stabilization

The wavelength locking method we have demonstrated serves as an effective means to initialize the microring-based photonic link. Once the link has been initialized, it is necessary to guard it against thermal fluctuations. Conventionally, to maintain the local temperature of the microring, the heat generated by the integrated heater is increased or decreased in response to decreases or increases in the ambient temperature [10].

To implement this, the thermal dithering system was cascaded with a feedback system (as schematized in Fig. 3) to thermally stabilize the microring resonator. To test the system, 10-Hz sinusoidal thermal fluctuations of magnitude 5 K were generated using an external visible laser [9].

In order to verify the thermal stabilization, wavelength scans were performed of a resonance adjacent in wavelength to the resonance that the thermal dithering & feedback system was locked to (see Fig. 11). As Fig. 11 shows, with the thermal dithering & feedback system implemented, the microring resonance stays locked to the laser wavelength, with the dynamic tuning of the heater counteracting the thermal fluctuations inflicted on the microring (see Fig. 12). In contrast, without thermal stabilization, the resonance fluctuates severely, being washed out in the wavelength scan (see Fig. 11).

This thermal stabilization method is robust enough that wavelength locking can occur even in thermally volatile environments. To demonstrate this the microring resonator was wavelength locked while the microring resonator was subjected to sinusoidal thermal fluctuations. Fig. 13 shows the heater voltage during this process. At the moment in time that the microring resonator is wavelength locked, the system immediately begins the thermal stabilization mechanism (as evidenced by the sinusoidal counter-tuning of the heater voltage in Fig. 13).

V. Scalability and Power Efficiency

In order for the demonstrated control system to be adapted for commercial microring-based links it must be scalable. Scalability requires meeting two criteria, the first being that the control system is sufficiently low-power such that the aggregate power consumption of initializing and stabilizing all the microring

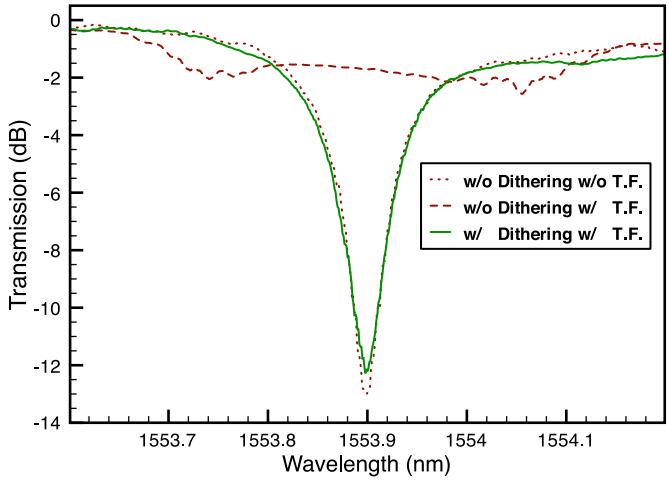

Fig. 11. The microring resonance when subjected to thermal fluctuations (T.F.), with and without the dithering & feedback system implemented. Also shown for comparison is the resonance without the stabilization system under normal, thermally stable conditions.

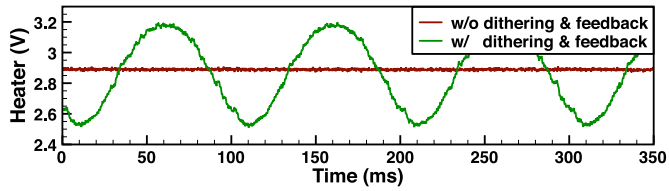

Fig. 12. Heater voltage when the microring resonator is being exposed to thermal fluctuations and, with and without, the dithering system actively counteracting said thermal fluctuations.

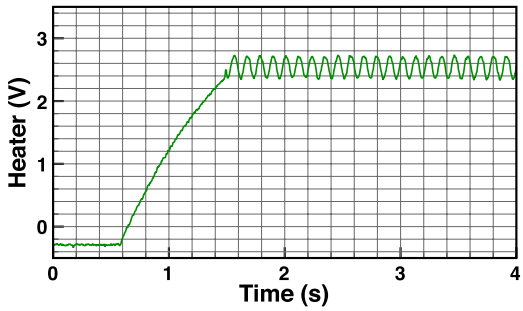

Fig. 13. Heater voltage as the microring resonator is wavelength locked while being subjected to sinusoidal thermal fluctuations.

resonators in the optical link does not exceed the power-efficiency improvement gained by the use of microring resonators. Secondly, the mechanisms in the control system must be compatible with the typical WDM configuration of microring resonators, in which they are cascaded along a common waveguide bus.

To get an estimate of the power consumption we replicate the approach of [10], tabulating the active components of the control circuitry (see Fig. 3) and referencing established power consumption figures when these components are implemented in conservative CMOS technology. We note that the majority of the circuitry devoted to wavelength locking (see Fig. 3, red box) is composed of digital logic elements that only draw power when switching logic states. Under the assumption that the optical link's operating time will be much longer than the initialization period, the power consumption of these elements are negligible. The feedback control can be decomposed into 4 op-amps [10], with the TIA, unity buffer, and summers contributing another 4 op-amps, for a total of 8 op-amps. Op-amps with the required $\sim$MHz bandwidth characteristics have routinely been implemented in CMOS technology with power consumptions as low as 40 μW [15]. The dithering signal can be implemented using an oscillator, with an example oscillator covering the required sub-MHz to few-MHz range while exhibiting power consumptions as low as 20 μW [16]. Lastly, analog multipliers are also routinely implemented in CMOS technology, with a conservative example having a power consumption of 45 μW [17]. The aggregate power consumption of the control circuitry can then be estimated to be 385 μW. To express this in the popular fJ/bit metric we assume that the microring resonator is operating on a 10 Gb/s data signal, yielding a power consumption of 38.5 fJ/bit for the control circuitry. This estimate falls well within the strictest pJ/bit power budgets required of some envisioned applications [1].

When evaluating the power consumption of this solution, the power consumption of the integrated heater should also be taken into consideration. However, this power consumption can be treated independently of the control circuitry, and will be a function of the heater efficiency, required tuning distance, and variation in temperature [10]. Advances in integrated heater design continue to improve on their efficiency [18]–[20], indicating that they will eventually adhere to the power consumption budget of microring-based optical links.

When considering the other important criteria, that the control method is compatible with WDM implementation, we note that there are no inherent features of the dithering technique that precludes the use of WDM. The dithering is a process local to the microring resonator and does not affect adjacent cascaded microring resonators. Additionally, by using different dithering frequencies for different microring resonators, the orthogonality principle can be leveraged (2)

$$\int \cos(f_n t)\cos(f_m t)dt = 0, f_n \neq f_m. \tag{2}$$

This feature eliminates crosstalk in error signals even when microring resonators overlap in the spectral regime. Hence, WDM implementation can be readily achieved, with each microring resonator in the cascaded array initializing and stabilizing independently.

VI. Conclusion

The demonstrated system has been shown to be able to effectively initialize and thermally stabilize individual microring resonators. Our experimental testbed limited us to testing the system against thermal fluctuations of magnitude 5 K. However, the temperature range an implemented solution could cover is much larger. There are no inherent limitations on the voltages supplied by the control circuitry, and integrated heaters typically have very large temperature tuning ranges (tested to be $>$80 K on our device). This should be sufficient to cover the

temperature variations in envisioned applications. For instance, within a data center rack, the projected temperature variation is at most 20 K [21].

As discussed, the novel use of thermal dithering to generate the error signal has the advantage of giving the feedback system relative immunity to power fluctuations. This renders the system robust against fluctuations in the received power, and resilient to Fabry-Perot artifacts in the optical path. Additionally, the use of low-speed analog and digital ICs in the experimental implementation lends credibility to the system's ability to scale in an energy-efficient manner to the multiple microring resonators that comprise a WDM photonic interconnect. Thus, the fabrication offset and thermal issues that currently plague microring resonators can be resolved in future commercial implementations, allowing them to be manifested in a variety of applications for the purpose of delivering magnitudes of order greater interconnect bandwidth than available with traditional electronic interconnects.

APPENDIX

The Fourier representation of a normalized 2π-periodic ideal square wave is given in (3)

$$f(t,\phi) = \frac{4}{\pi} \sum_{n=1,3,5\ldots}^{\infty} \frac{\sin(nt+\phi)}{n}. \tag{3}$$

As per the construction given in Section I, when the generated optical modulation is in-phase with the driving dithering signal, the product is given as (4)

$$f(t,0)f(t,0) = \frac{16}{\pi^2}\left(\sum_{n=1,3,5\ldots}^{\infty} \frac{\sin(nt)}{n}\right)\left(\sum_{n=1,3,5\ldots}^{\infty} \frac{\sin(nt)}{n}\right). \tag{4}$$

The DC component is given as the integral of (4). Using the orthogonality principle (2), the cross-terms can be eliminated, leaving the non-zero terms given in (5)

$$\begin{aligned}\int f(t,0)f(t,0)dt &= \frac{16}{\pi^2}\int \sum_{n=1,3,5\ldots}^{\infty} \frac{\sin^2(nt)}{n^2}dt \\ &= \frac{16}{\pi^2}\left(\frac{1}{2}\right)\sum_{n=1,3,5\ldots}^{\infty}\frac{1}{n^2} \\ &= \frac{16}{\pi^2}\left(\frac{1}{2}\right)\left(\frac{\pi^2}{8}\right) = 1\end{aligned} \tag{5}$$

where the infinite summation has been solved as a modified Basel series. Similarly, when the generated optical modulation is out-of-phase with the driving dithering signal, the product and dc component are given as (6) and (7), respectively,

$$\begin{aligned}f(t,0)f(t,\pi) = \frac{16}{\pi^2}&\left(\sum_{n=1,3,5\ldots}^{\infty} \frac{\sin(nt)}{n}\right) \\ &\times \left(\sum_{n=1,3,5\ldots}^{\infty} \frac{\sin(nt+\pi)}{n}\right)\end{aligned} \tag{6}$$

$$\int f(t,0)f(t,\pi)dt = -\frac{16}{\pi^2}\int \sum_{n=1,3,5\ldots}^{\infty} \frac{\sin^2(nt)}{n^2}dt = -1. \tag{7}$$

Hence, the dc component takes on a value of $\{1,-1\}$, in comparison to using normalized sinusoidal waves (section I), in which the dc components have values of $\{1/2, -1/2\}$.

ACKNOWLEDGMENT

The authors gratefully acknowledge R. Grote for his group index calculation. Additionally, the authors are also grateful to CMC Microsystems and IME Singapore for enabling work in the design and fabrication of the silicon photonic chips.

REFERENCES

[1] A. V. Krishnamoorthy, R. Ho, X. Zheng, H. Schwetman, J. Lexau, P. Koka, G. Li, I. Shubin, and J. E. Cunningham, "Computer systems based on silicon photonic interconnects," *Proc. IEEE*, vol. 97, no. 7, pp. 1337–1361, Jul. 2009.

[2] R. Urata, H. Liu, C. Lam, P. Dashti, and C. Johnson, "Silicon photonics for optical access networks," in *Proc. IEEE 9th Int. Conf. Group IV Photonics*, 2012, pp. 207–209.

[3] N. Ophir, D. Mountain, C. Mineo, and K. Bergman, "Silicon photonic microring links for high-bandwidth-density, low-power chip I/O," *IEEE Micro*, vol. 33, no. 1, pp. 45–67, Jan./Feb. 2013.

[4] J. Chan and K. Bergman, "Photonic interconnection network architectures using wavelength-selective spatial routing for chip-scale communiations," *J. Opt. Commun. Netw.*, vol. 4, no. 3, pp. 189–201, 2012.

[5] A. W. Poon, X. Luo, F. Xu, and H. Chen, "Cascaded microresonator-based matrix switch for silicon on-chip optical interconnection," *Proc. IEEE*, vol. 97, no. 7, pp. 1216–1238, Jul. 2009.

[6] J. E. Cunningham, I. Shubin, X. Zheng, T. Pinguet, A. Mekis, Y. Luo, H. Thacker, G. Li, J. Yao, K. Raj, and A. V. Krishnamoorthy, "Highly-efficient thermally-tuned resonant optical filters," *Opt. Exp.*, vol. 18, no. 18, pp. 19055–19063, 2010.

[7] E. Timurdogan, A. Biberman, D. C. Trotter, C. Sun, M. Morseco, V. Stojanovic, and M. R. Watts, "Automated wavelength recovery for microring resonators," in *Proc. Conf. Lasers Electro-Opt.*, 2012, pp. 1–2.

[8] W. A. Zortman, A. L. Lentine, D. C. Trotter, and M. R. Watts, "Bit error monitoring for active wavelength control of silicon microphotonic resonant modulators," *IEEE Micro*, vol. 33, no. 1, pp. 42–52, Jan./Feb. 2013.

[9] K. Padmaraju, J. Chan, L. Chen, M. Lipson, and K. Bergman, "Thermal stabilization of a microring modulator," *Opt. Exp.*, vol. 20, no. 27, pp. 27999–28008, 2012.

[10] K. Padmaraju, D. F. Logan, X. Zhu, J. J. Ackert, A. P. Knights, and K. Bergman, "Integrated thermal stabilization of a microring modulator," *Opt. Exp.*, vol. 21, no. 12, pp. 14342–14350, 2013.

[11] J. A. Cox, D. C. Trotter, and A. L. Starbuck, "Integrated control of silicon-photonic micro-resonator wavelength with balanced homodyne locking," in *Proc. Conf. Laser Electro-Opt.*, 2013, pp. 52–53.

[12] K. Padmaraju, D. F. Logan, J. J. Ackert, A. P. Knights, and K. Bergman, "Microring resonance stabilization using thermal dithering," in *Proc. IEEE Opt. Interconnects Conf.*, 2013, pp. 58–59.

[13] R. W. P. Drever, J. L. Hall, F. V. Kowalski, J. Hough, G. M. Ford, A. J. Munley, and H. Ward, "Laser phase and frequency stabilization using an intracavity etalon," *Appl. Phys. B.*, vol. 31, no. 2, pp. 97–105, 1983.

[14] D. F. Logan, P. Velha, M. Sorel, R. M. De La Rue, P. E. Jessop, and A. P. Knights, "Monitoring and tuning micro-ring properties using defect-enhanced silicon photodiodes at 1550 nm," *IEEE Photon. Technol. Lett.*, vol. 24, no. 4, pp. 261–263, Feb. 2012.

[15] C. J. B. Fayomi, M. Sawan, and G. W. Roberts, "Reliable circuit techniques for low-voltage analog design in deep submicron standard CMOS: a tutorial," *Analog Integr. Circuits Signal Process*, vol. 39, no. 1, pp. 21–38, 2004.

[16] K. Lasanen, E. Raisanen-Ruotsalainen, and J. Kostamovaara, "A 1-V, Self-adjusting, 5-MHz CMOS RC-Oscillator," in *Proc. IEEE Int. Symp. Circuits Syst.*, 2002, pp. 377–380.

[17] C. Chen and Z. Li, "A low-power CMOS analog multiplier," *IEEE Trans. Circuits Syst., II, Exp. Briefs*, vol. 53, no. 6, pp. 100–104, Feb. 2006.

[18] P. Dong, W. Qian, H. Liang, R. Shafiiha, D. Feng, G. Li, J. E. Cunningham, A. V. Krishnamoorthy, and M. Asghari, "Thermally tunable silicon racetrack resonators with ultralow tuning power," *Opt. Exp.*, vol. 18, no. 19, pp. 20298–20304, 2010.
[19] Q. Fang, J. Song, X. Luo, L. Jia, M. Yu, G. Lo, and Y. Liu, "High efficiency ring-resonator filter with nisi heater," *IEEE Photon. Technol. Lett.*, vol. 24, no. 5, pp. 350–352, Mar. 2012.
[20] M. R. Watts, W. A. Zortman, D. C. Trotter, G. N. Nielson, D. L. Luck, and R. W. Young, "Adiabatic resonant microrings (ARMs) with directly integrated thermal microphotonics," in *Proc. Conf. Lasers Electro-Opt.*, 2009, pp. 1–2.
[21] R. R. Schmidt, E. E. Cruz, and M. K. Iyengar, "Challenges of data center thermal management," *IBM J. Res. Develop.*, vol. 49, no. 4/5, pp. 709–723, 2005.

Kishore Padmaraju (S'07) received the B.S. degree (highest distinction) in electrical and computer engineering from the University of Rochester, Rochester, NY, USA, in 2009, and the M.S. degree in electrical engineering from Columbia University, New York, NY, USA, in 2011, where he is currently working toward the Ph.D. degree in the Department of Electrical Engineering.

His current research interests include control systems for the initialization and stabilization of silicon photonics devices, as well as the use of silicon photonic devices for advanced modulation formats in optical communication systems.

Dylan F. Logan received the B.Eng. and Ph.D. degrees in engineering physics from McMaster University, Hamilton, ON, Canada, in 2007 and 2011, respectively.

He recently completed a postdoctoral fellowship at the University of Toronto, where he worked in integrated waveguide nonlinear optics. He is currently a Design Engineer with Ranovus Inc., Ottawa, ON, Canada. His research interests include silicon photonic device design and transceiver architectures.

Takashi Shiraishi (M'07) received the B.S. and the M.S. degrees from the Tsukuba University, Ibaraki, Japan, in 2000 and 2002, respectively, all in science and engineering.

He is currently working as a Visiting Researcher with the Department of Electrical Engineering, Columbia University, New York, NY, USA, and also with the Photonics Laboratory, Fujitsu Laboratories Ltd., Kanagawa, Japan. His current research focuses on the application of silicon photonic optical networks to memory systems.

Jason J. Ackert received the B.Sc. degree in physics from the University of Waterloo, Waterloo, ON, Canada, in 2009. He is currently working toward the Ph.D. degree in the Department of Engineering Physics, McMaster University, Hamilton, ON, Canada.

His current research focuses on monolithically integrated silicon photonic devices and their application to optical interconnects.

Andrew P. Knights received the Ph.D. degree from the University of East Anglia, Norwich, U.K., in 1994 in the area of surface and subsurface material characterization.

His subsequent work took him first to the University of Western Ontario, London, ON, Canada, where he performed research on the generation and evolution of implant induced defects in silicon, and then to the University of Surrey, Surrey, U.K., as part of the U.K. National Ion Beam Centre, researching novel fabrication processes for micro- and opto-electronic materials. In 2000, he joined Bookham Technology and worked on a range of silicon-based, highly integrated photonic devices. In 2003, he moved to McMaster University, Hamilton, ON, Canada, where he holds a faculty position with the Department of Engineering Physics. He currently leads a research group working on the interaction of optical and electrical functionality in silicon-based structures.

Keren Bergman (S'87–M'93–SM'07–F'09) received the B.S. degree from Bucknell University, Lewisburg, PA, USA, in 1988, and the M.S. and Ph.D. degrees from the Massachusetts Institute of Technology, Cambridge, MA, USA, in 1991 and 1994, respectively, all in electrical engineering.

She is currently the Charles Batchelor Professor and Chair of Electrical Engineering at Columbia University, New York, NY, USA, where she also directs the Lightwave Research Laboratory. She leads multiple research programs on optical interconnection networks for advanced computing systems, data centers, optical packet switched routers, and chip multiprocessor nanophotonic networks-on-chip.

Dr. Bergman is a Fellow of the Optical Society of America. She currently serves as the CoEditor-in-Chief of the *IEEE/OSA Journal of Optical Communications and Networking*.